JET–P(99)30

D Testa
A Gondhalekar

Fast Ion Density Measurements using High Energy Neutral Particle Analysis in JET

JET–P(99)30

Fast Ion Density Measurements using High Energy Neutral Particle Analysis in JET

D Testa[1,2], A Gondhalekar.

JET Joint Undertaking, Abingdon, Oxfordshire, OX14 3EA,
[1]Imperial College of Science, Technology and Medicine, London, SW7 2BZ, UK.
[2]Permanent address: Massachusetts Institute of Technology,
Plasma Science and Fusion Centre, Cambridge, MA02139, USA.

Preprint of a Paper to be submitted for publication in Nuclear Fusion

September 1999

ABSTRACT

In the JET tokamak the perpendicular velocity distribution function of Ion Cyclotron Resonance Frequency (ICRF) heated ions is inferred in the energy range $0.3 \leq E(MeV) \leq 1.5$ from Neutral Particle Analyser (NPA) measurements of the emitted high energy atomic flux. The measurement is integrated along a vertical line-of-sight through the plasma centre, with a finite viewing solid angle. We present a method to deduce the ICRF heated minority ion density in the plasma centre taking into full consideration the geometry of the measurement. We verify our results against independent measurements of the fast ion density and perpendicular energy content, and we obtain quantitative agreement. Our results further validate the model of impurity-induced neutralisation, which was developed to interpret the high energy atomic flux measurements in JET. They give access to a fundamental property of the ICRF-heated ion distribution function, and provide improved tools for understanding the behaviour of fast ion populations in forthcoming fusion experiments.

1. INTRODUCTION

Neutral Particle Analysis (NPA) is a well-known technique for measuring the flux of atoms escaping from the plasma and thus deducing the energy distribution function of plasma ions [1,2]. High energy NPA measurements have become well established in JET for determining the energy distribution function of Ion Cyclotron Resonance Frequency (ICRF) heated ions [3,4,5,6] and of charged fusion products [7]. The measurements are non-perturbing and rely on passive neutralisation of the ions by one and two-electron species of the main intrinsic plasma impurities [8]. In this Impurity Induced Neutralisation (IIN) model the population of partially ionised impurity ions is sustained in high temperature thermonuclear plasmas by hydrogen isotope atoms due to recycling at the first wall or Neutral Beam Injection (NBI).

For the high power densities and long slowing-down times achieved in present-days experiments, the distribution function of ICRF heated ions becomes strongly anisotropic, with perpendicular temperature much higher than the parallel temperature, and significantly greater than that of non-resonating plasma species. These high energy anisotropic ion populations can significantly enhance the fusion yield above that of a thermal isotropic plasma for the same total energy content, and may also stabilise sawteeth and low frequency MHD modes [3,4,9,10]. Measurements of ICRF heated ion distribution function are required for several reasons, such as to provide experimental testing and validation of theories on ICRF heating of fusion plasmas, and to quantify the observed link between fast ions and MHD instabilities.

Purpose of our work is to infer the energy distribution function of ICRF-heated ions and extend the analysis given in [5]. In this previous work it was shown how to deduce the peak perpendicular temperature of ICRF-heated protons from the NPA measurements: to this end, only the energy dependence of the emitted atomic flux is required. However, to infer the density in the plasma centre of such ions, also the absolute calibration of the NPA is needed, which is

given by fully considering the geometry of its line-of-sight. In this paper we derive a general analytic expression for the absolute calibration of the atomic flux detected by the NPA during ICRF heating of JET plasmas. For these experiments the distribution function of such ions can be well approximated with a bi-Maxwellian, with perpendicular temperature $T_\perp$ much greater than the parallel temperature $T_{||}$ [5,6]. Thus we are able to deduce the fast ion density n_{FAST} from the absolute calibration of the NPA when $T_\perp$ and $T_{||}/T_\perp$ are both known. We use for $T_\perp$ and $T_{||}/T_\perp$ the expressions given in [5,6].

In this work we analyse JET experiments with central ICRF heating of deuterium plasmas containing minority protons and high energy deuterons due to NBI. The ICRF system is tuned to deuterium 2nd cyclotron harmonic heating in the plasma centre, which coincides with the 1st harmonic of the protons. We verify our results against independent measurements of fast ion density and magnetic measurement of the total fast ion perpendicular energy content. We obtain quantitative agreement within the accuracy of the measurements. Our results further validate the IIN model [8], which was developed to interpret the high energy atomic flux measurements in JET.

This paper is organised as follows. Section 2 gives a brief description of the high energy NPA used for the measurements of the fast ion perpendicular velocity distribution function. Section 3 presents the method used to infer the minority ICRF-heated ion density using the NPA measurements. In Section 4 we compare our results with independent measurements of the fast ion density and perpendicular energy content. In Section 5 we present our conclusions.

2. THE HIGH ENERGY NPA

The NPA is of the conventional $E||B$ type, and is located on the torus with its vertical line-of-sight intersecting the plasma at a major radius $R_{NPA}=3.07m$. The projection area of the collimator on the plasma mid-plane is $A_{NPA}=3\times10^{-3}m^2$, and the viewing solid angle is $\phi_{NPA}=1.18\times10^{-6}sterad$. The line-of-sight geometry determines that only ions with $\upsilon_z/\upsilon_{||}\geq200$ can be detected by the NPA. Here $\upsilon_{||}$ is the velocity in the toroidal mid-plane, which is very close to the velocity parallel to the toroidal magnetic field, and υ_z is the vertical velocity, perpendicular to the toroidal mid-plane. The NPA can detect time resolved atomic fluxes of hydrogen (H), deuterium (D), tritium (T), helium3 (^{3}He) and alpha particles (^{4}He) in the energy range $0.2\leq E(MeV)\leq3.5$. There are eight energy channels with common charge and mass selection, thus only one ion species can be measured at a time. Further details of the measurement technique and experimental set-up are given in [6,8,11].

3. INTERPRETATION OF THE NPA MEASUREMENTS

The quantity measured by the NPA is the flux of atoms $\Gamma_{MEAS}(E_z)$ escaping the plasma perpendicularly to the toroidal magnetic field per unit time per unit area per unit energy. It is proportional to the line integral of the local energy distribution function $F(E_z,z)$ weighted with respect to the local neutralisation probability $P_N(E,z)$

$$\Gamma_{MEAS}(E_z) = \int_{-b}^{b} dz P_V(E,z) F(E_z,z) \ . \tag{1}$$

Here E is the energy of the atoms, z is the vertical co-ordinate and b is the plasma height along the line-of-sight. P_V depends on neutralisation cross-sections, is a complicated function of plasma parameters, and has a scale length of the order of b. F depends on ICRF wave dispersion, with a scale length of the order of the Doppler width of the resonance $\Delta << b$. Thus we approximate $P_V(E,z) \approx P_V(E,0)$ and define a line integrated distribution function $F_{MEAS}(E_z)$

$$F_{MEAS}(E_z) = \frac{\Gamma_{MEAS}(E_z)}{P_V(E,0)} \approx \int_{-b}^{b} dz F(E_z,z) \ . \tag{2}$$

In the energy range of the measurements it is possible to adopt [5,6] a bi-Maxwellian model for the local velocity distribution function of the ICRF-heated ions $f(\upsilon_x,\upsilon_y,\upsilon_z;r,z)$

$$f(\upsilon_x,\upsilon_y,\upsilon_z;r,z) = \left(\frac{m}{2\pi}\right)^{3/2} \frac{n(r,z)}{T_{||}^{1/2}(r,z) T_{\perp}(r,z)} exp\left[-\frac{m\upsilon_x^2}{2T_{||}(r,z)} - \frac{m(\upsilon_y^2+\upsilon_z^2)}{2T_{\perp}(r,z)}\right] . \tag{3}$$

Here n and m are density and mass of the measured ion species, $T_{||}$ and $T_{\perp}$ are the parallel and perpendicular temperature, the x co-ordinate is along the toroidal magnetic field, the y and z-co-ordinates define the poloidal plane and $r=(x^2+y^2)^{1/2}$ is the radial co-ordinate in the toroidal mid-plane. Because the velocity vector of an ion is not significantly affected by electron capture due to the ion-electron mass ratio, the velocity distribution function $f(\upsilon_z;r,z)$ of the ions which, if neutralised, are detected by the NPA, is given by

$$f(\upsilon_z;r,z) = \iint d\upsilon_x d\upsilon_y f(\upsilon_x,\upsilon_y,\upsilon_z;r,z) = \int_0^{2\pi} d\phi \int_0^{\upsilon_z/200} d\upsilon_\phi \upsilon_\phi f(\upsilon_\phi,\phi,\upsilon_z;r,z) \ , \tag{4}$$

$$f(\upsilon_\phi,\phi,\upsilon_z) = \left(\frac{m}{2\pi}\right)^{3/2} \frac{n}{T_{||}^{1/2} T_{\perp}} exp\left\{-\frac{m\upsilon_\phi^2}{2T_{\perp}}\left[1+\left(\frac{T_{\perp}}{T_{||}}-1\right)cos^2\phi\right] - \frac{m\upsilon_z^2}{2T_{\perp}}\right\} . \tag{5}$$

Here $\upsilon_\phi=(\upsilon_x^2+\upsilon_y^2)^{1/2}$ is the toroidal velocity, $\phi=arctg(\upsilon_y/\upsilon_x)$ is the toroidal angle and the condition on υ_Z is set by the viewing solid angle. Using now eq.[5] in eq.[4] to perform the integral over (υ_ϕ,ϕ) and expand $f(\upsilon_z;r,z)$ in terms of the pitch angle υ_z/υ_ϕ, we have [6]

$$\begin{aligned} f(\upsilon_z;r,z) &= \frac{n(r,z)\alpha(r,z)}{4\pi}\left[\frac{m}{2\pi T_{||}(r,z)}\right]^{1/2} exp\left[-\frac{m\upsilon_z^2}{2T_{\perp}(r,z)}\right] \times \\ &\times \sum_{q=0}^{\infty} (-1)^q \frac{(4q+1)\Gamma^3(q+1/2)}{\Gamma(2q+3/2)\Gamma^2(q+1)} \int_0^{\rho_0} d\rho \rho^q e^{-\alpha(r,z)\rho} M\left(q+\frac{1}{2}, 2q+\frac{3}{2}; -\rho\right) \end{aligned} \ . \tag{6}$$

Here M are Confluent Hypergeometric functions, Γ are Gamma functions, and we used

$$\int_0^\infty dx x^\mu e^{-\alpha x^2} J_\nu(\beta x) = \frac{\beta^\nu \Gamma[(\nu+\mu+1)/2]}{2^{\nu+1}\alpha^{(\nu+\mu+1)/2}\Gamma(\nu+1)} M\left(\frac{\nu+\mu+1}{2}, \nu+1; -\frac{\beta^2}{4\alpha}\right),$$

$$exp(-a^2\cos^2\phi) = Re\left\{\frac{2}{\sqrt{\pi}}\int_0^\infty dk\, exp(-k^2 + 2iak\cos\phi)\right\},$$

$$exp(iz\cos\phi) = \left(\frac{\pi}{2z}\right)^{1/2} \sum_{q=0}^{\infty} i^q (2q+1) J_{q+1/2}(z) P_q(\cos\phi)\ ,\ \int_0^{2\pi} d\phi P_{2q}(\cos\phi) = \frac{\Gamma^2(q+1/2)}{\Gamma^2(q+1)}\ .$$

Here J_μ are Bessel functions of 1st kind and P_q Legendre Polynomials. In eq.[6] $\alpha=T_{||}/(T_\perp-T_{||})$ defines the anisotropy of the fast ion distribution function and $\rho_0=1.25x10^{-5} m\upsilon_z^2/\alpha T_\perp$ is the expansion parameter. From eq.[6] we notice that the geometrical constraints imposed on the measured atomic flux by the finite aperture of the vertical viewing solid angle translate into physical constraints on the velocity phase-space of the deduced line-integrated distribution function, which is no more Maxwellian in the vertical velocity. For JET plasmas in the energy range of the measurements we have $T_\perp<E_z=m\upsilon_z^2/2<10^2 T_\perp$, thus we analytically approximate $f(\upsilon_z;r,z)$ by considering only the first two terms in eq.[6]. Using phase-space conservation $f(\upsilon_z;r,z)d\upsilon_z=F(E_z;r,z)dE_z$ and $\nu=6.25x10^{-6}(1+T_\perp/T_{||})<10^{-4}$ for JET experiments, we obtain the energy distribution function [6]

$$F(E_z;r,z) = \frac{n(r,z)}{4(200)^2 T_\perp(r,z)}\left[\frac{E_z}{\pi T_{||}(r,z)}\right]^{1/2} exp\left[-\frac{E_z}{T_\perp(r,z)}\right]\left[1-\frac{\nu(r,z)E_z}{T_\perp(r,z)}\right]. \qquad (7)$$

To obtain eq.[7], we used the following relations, where γ is the incomplete Gamma function:

$$M(a,b;z) = \sum_{q=0}^{\infty} \frac{(a)_q z^q}{(b)_q q!}\ ,\ (a)_q = a(a+1)(a+2)\ldots(a+q-1)\ ,$$

$$(a)_0 = 1\ ,$$

$$\int_0^x dt t^{a-1} e^{-t} = \gamma(a,x) = \sum_{q=0}^{\infty} \frac{(-1)^q x^{a+q}}{(a+q)q!}\ .$$

The spatial profile of the ICRF-heated distribution function was taken in [5] to depend only on z but not on r. This approach corresponds to neglecting the finite viewing area of the NPA in the

toroidal mid-plane, thus assuming that the measured neutral flux comes only from a single line. However, it can be shown [1,2,6] that both the density and temperature spatial profiles of ICRF-heated ions can be well modelled by gaussian expressions such as

$$T_{\perp}(r,z) = T_0\, exp\left(-\frac{r^2}{d^2} - \frac{z^2}{l^2}\right), \qquad \xi(r,z) = \frac{T_{||}(r,z)}{T_{\perp}(r,z)}, \qquad n(r,z) = n_0\, exp\left(-\frac{r^2}{\delta^2} - \frac{z^2}{\lambda^2}\right)$$

Here $\xi(r,z)$ defines the ratio between parallel and perpendicular temperature, and in most cases we can assume a constant $\xi(r,z)=\xi_0$, taken in the plasma centre. The finite aperture of the viewing solid angle allows ions with the proper pitch-angle to enter the NPA only if they are neutralised at a radial position $|R-R_{NPA}|\leq r_0$. Here $r_0 \approx 5.5cm$ is the projection of the vertical viewing solid angle in the mid-plane. Therefore the line integral of the surface average of $F(E_z;r,z)$ corresponds to the measured distribution function

$$F_{MEAS}(E_z) = \frac{1}{\Phi_{NPA} A_{MID}} \iint dA dz F(E_z;r,z)\Theta(r_0 - r) \; . \tag{8}$$

Here the step function $\Theta(r_0-r)$ selects only ions neutralised in the viewing solid angle Φ_{NPA} to be detected by the NPA. A_{MID} is the viewed mid-plane area and can be calculated considering that the NPA is measuring in one octant of the JET torus, thus $A_{MID}=(2\pi R_0)(2a)/8=\pi a R_0/2$, where R_0 is the plasma geometric centre and a is horizontal minor radius. Replacing now $\nu(r,z)$ with its value in the plasma centre $\nu_0=6.25x10^{-6}(1+1/\xi_0)$, eq.[8] becomes

$$F_{MEAS}(E_z) = C_0 \int_0^{x0} dx\, exp(-\varepsilon_1 x) I(\nu_0, \beta, \varepsilon_2) \; . \tag{9}$$

The normalisation constant C_0, the function $I(\nu_0,\beta,\varepsilon_2)$ and the coefficients $(\beta,\varepsilon_1,\varepsilon_2)$ are

$$C_0 = \frac{n_0 l d^2}{2(200)^2 T_0 A_{MID} \Phi_{NPA}} \left(\frac{\pi E_z}{\xi T_0}\right)^{1/2}, \; I(\nu_0,\beta,\varepsilon_2) = \int_0^{t0} dt\, exp\left(-\beta e^{t^2} - \varepsilon_2 t^2\right)\left(1 - \nu_0 \beta e^{t^2}\right),$$

$$\beta = \frac{E_z e^x}{T_0}, \; \varepsilon_1 = \frac{d^2}{\delta^2} - \frac{3}{2}, \; \varepsilon_2 = \frac{l^2}{\lambda^2} - \frac{3}{2}, \; x_0 = \frac{r_0^2}{d^2}, \; t_0 = \frac{b}{l} \; .$$

In JET the vertical minor radius $b=2.1m$, for typical plasmas $l \approx \lambda \approx 0.3m$ so that $t_0 \approx 7$: thus we can replace the finite interval of integration in $I(\nu_0,\beta,\varepsilon_2)$ by a semi-infinite one. Moreover, for large values of β, corresponding to supra-thermal energies $E_z/T_0>3$, it has been shown [5] that $F_{MEAS}(E_z)/(E_z/T_0)^{1/2} \approx exp(-E_z/T_0)$. Expanding $exp(t^2) \approx 1+t^2+t^4/2$ in $I(\nu_0,\beta,\varepsilon_2)$, the integral is analytically tractable and reads [6]

$$I(\upsilon_0,\beta,\varepsilon_2)\approx\sqrt{\frac{z_1}{8}}\,exp\left(\frac{\beta z_1^2}{4}-\beta\right)K_{1/4}\left(\frac{\beta z_1^2}{4}\right)-\nu_0\beta\sqrt{\frac{z_2}{8}}\,exp\left(\frac{\beta z_2^2}{4}-\beta\right)K_{1/4}\left(\frac{\beta z_2^2}{4}\right). \quad (10)$$

Here $z_1=1+\varepsilon_2/\beta$, $z_2=1+(\varepsilon_2-1)/\beta$, $K_{1/4}$ are modified Bessel functions of second kind and

$$\int_0^\infty dx\,exp(-\beta^2x^4-2\gamma^2x^2)=\frac{\gamma}{\sqrt{8}\beta}exp\left(\frac{\gamma^4}{2\beta^2}\right)K_{1/4}\left(\frac{\gamma^4}{2\beta^2}\right).$$

Using the asymptotic expansion for large argument for $K_{1/4}$ in $I(\nu_0,\beta,\varepsilon_2)$, eq.[10] reads

$$K_\nu(z)\xrightarrow[|z|>>1]{}\sqrt{\frac{\pi}{2z}}e^{-z}\sum_{q=0}^{\infty}\frac{(\kappa)_q}{(8z)^q\,q!}\ ,\ (\kappa)_q=(4\nu^2-1)\ldots[4\nu^2-(2q-1)^2]\ ,$$

$$(\kappa)_0=1\ ,$$

$$F_{MEAS}(E_z)=C_0\int_0^{x0}dx\,exp(-\beta-\varepsilon_1x)\beta^{-1/2}\left(1-\frac{3+4\varepsilon_2}{8\beta}-\nu_0\beta\right)=$$

$$=\frac{C_0x_0}{4}\sqrt{\frac{\pi T_0}{E_z}}\,exp\left(-\frac{E_z}{T_0}\right)\sum_{q=0}^{\infty}\frac{(-1)^q}{\Gamma(q)}\left(\frac{x_0^2\tau}{2}\right)^q\left[2H_q(w_1)-\frac{3+4\varepsilon_2}{2\tau^2}H_q(w_2)-\nu_0\tau^2H_q(w_3)\right] \quad (11)$$

Here $\tau=(E_z/2T_0)^{1/2}$, $w_1=(\varepsilon_1+1/2+\tau^2/2)/\tau$, $w_2=(\varepsilon_1+3/2+\tau^2/2)/\tau$, $w_3=(\varepsilon_1-1/2+\tau^2/2)/\tau$ and H_q are Hermite Polynomials, and we kept only first order terms from eq.[10]. To deduce eq.[11] we used the definition of the error function *erf(z)* and expanded it to first order in term of its Taylor series involving H_q

$$\int_0^u dx\,exp\left(-x\gamma-\frac{x^2}{4\beta}\right)=\sqrt{\pi\beta}\,exp(\beta\gamma^2)\left[erf\left(\gamma\sqrt{\beta}+\frac{u}{2\sqrt{\beta}}\right)-erf\left(\gamma\sqrt{\beta}\right)\right],$$

$$\frac{d^{q+1}}{dz^{q+1}}erf(z)=(-1)^q\frac{2e^{-z^2}}{\sqrt{\pi}}H_q(z)\ ,$$

$$H_q(x)=(-1)^qe^{x^2}\frac{d^q}{dx^q}\left(e^{-x^2}\right).$$

For typical JET plasmas $d\approx\delta\approx0.3m$ and the expansion parameter in the series defining eq.[11] is $x_0^2\tau/2\approx8x10^{-4}(E_z/T_0)^{1/2}<<1$. Considering the first two terms in eq.[11], the measured line integrated surface average ICRF-heated ion distribution function reads [6]

$$F_{MEAS}(E_z) = \frac{\pi r_0^2 l}{4(200)^2 \sqrt{\xi} A_{MID} \Phi_{NPA}} \frac{n_0}{T_0} exp\left(-\frac{E_z}{T_0}\right) \times$$
$$\times \left[1 - \frac{(2\nu_0 + x_0)E_z}{2T_0} - \frac{(4\varepsilon_2 + 3)T_0}{8E_z} - \frac{(8\varepsilon_1 - 4\varepsilon_2 + 1)x_0}{16}\right] = , \qquad (12)$$
$$= \frac{\sigma_0 n_0}{T_0 A_{MID}} exp\left(-\frac{E_z}{T_0}\right)\left(1 - \frac{\sigma_1 E_z}{T_0} - \frac{\sigma_2 T_0}{E_z} - \sigma_3\right)$$

$$\xi_0 = \frac{T_{||0}}{T_{\perp 0}} \ , \ \nu_0 = \frac{1 + 1/\xi_0}{4(200)^2} \ , \ \varepsilon_1 = \frac{d^2}{\delta^2} - \frac{3}{2} \ , \ \varepsilon_2 = \frac{l^2}{\lambda^2} - \frac{3}{2} \ , \ x_0 = \frac{r_0^2}{d^2} \ .$$

$$\sigma_0 = \frac{\pi r_0^2 l}{4(200)^2 \sqrt{\xi} \Phi_{NPA}} \ , \ \sigma_1 = \nu_0 + \frac{x_0}{2} \ , \ \sigma_2 = \frac{4\varepsilon_2 + 3}{8} \ , \ \sigma_3 = \frac{(8\varepsilon_1 - 4\varepsilon_2 + 1)x_0}{16} \ .$$

This distribution function shows the usual Maxwellian behaviour in the leading order term. It has been derived using the fact that the energy range of the measurements is well above the peak fast ion temperature. We considered first order corrections for the pitch-angle spreading in the measured flux (terms containing ν_0), for the viewing solid angle finite aperture (x_0) and for the line-of-sight integration (T_0/E_z). Due to the expansion criteria used in the derivation, eq.[12] is valid for typical JET plasmas for $E_z/T_0 \leq 3.5x10^2$ when all corrections to the leading order term are vanishingly small. From inspection of eq.[11] it can be shown that the larger correction is given by $(x_0/2)(E_z/T_0) \approx 1.7x10^{-2}(E_z/T_0)$, which sets the limits of validity of eq.[12] to $3 < E_z/T_0 < 60$. This condition is satisfied in JET ICRF heating experiments since the typical peak fast ion temperature is in the range $100 < T_0(keV) < 600$ and for the NPA measurements considered in this paper we have $0.3 < E_z(MeV) < 1.5$.

In [5] a different form was given for $F_{MEAS}(E_z)$, which neglects surface average on the toroidal mid-plane and first order corrections in pitch-angle, and the normalisation C_0 for $F_{MEAS}(E_z)$ was not explicitly computed. Doing so shows that it would have been $C_0 \approx A_{MID}/\pi r_0^2 \approx 500$ times greater than that computed here, giving a peak fast ion density $n_0 \approx 500$ times smaller than the correct one. Conversely, no appreciable difference is found for the peak fast ion temperature T_0, since the leading order term is still Maxwellian and pitch-angle corrections are vanishingly small. These results can be understood considering that the aperture of the viewing solid angle allows atoms coming from a finite region in the toroidal mid-plane to enter the NPA, thus affecting the intensity of the measurement but not its energy distribution.

The surface average of the line-integrated ICRF-heated energy distribution function $F_{MEAS}(E_z)$ is given, with the proper normalisation constant, in terms of the unknown peak fast ion density n_0 and perpendicular temperature T_0, whereas all other parameters in eq.[12] can be determined from independent measurements and calculations. Because $F_{MEAS}(E_z)$ is not a simple Maxwellian in its energy distribution, the peak fast ion temperature can be defined as an

energy dependent quantity and calculated at the median energy in the measured range $<E_z>=E_*$ using $G(E_z)=F_{MEAS}(E_z)/\sqrt{E_z}$ by writing [5]

$$T_0 = -T(E_*)\left[\frac{d\ln G(E_z)}{d(E_z)}\right](@E_z = E_*) \ . \tag{13}$$

Here $T(E_*)$ is the temperature deduced from the leading order Maxwellian term of eq.[12]. At first order in $T(E_*)/E_*$ eq.[13] reduces to the same results given in [5]

$$T_0 = T(E_*)\left[1+\frac{T(E_*)}{2E_*}\right] . \tag{14}$$

Using eq.[14] and the geometrical factors entering the definition of $F_{MEAS}(E_z)$, eq.[12], we deduce the peak fast ion density n_0 by numerically computing the integral of $F_{MEAS}(E_z)$, eq.[12], over the energy range of the measurement [6], and we obtain

$$n_0 = \frac{1}{E_{MAX}-E_{MIN}}\int_{E_{MIN}}^{E_{MAX}} dEF_{MEAS}(E) \ . \tag{15}$$

We verify the approximation used to obtain eq.[12] by solving eq.[6] to different orders in its series expansion. It is worthwhile noticing that the accuracy of our computational approach has to be compared with the uncertainty in the NPA measurements of the absolute atomic flux, estimated to be ≈30% [6]. Fig.1 shows the comparison between three different estimates of the fast deuteron density n_{DFAST} inferred from the NPA measurements during combined ICRF+NBI heating obtained: (a) by solving eq.[12], (b) by solving eq.[6] to the order $q=10$, and (c) by solving eq.[6] to the order $q=200$. We notice that no appreciable difference in the inferred n_{DFAST} is obtained within the uncertainties of the NPA measurements using (a) and (b). We attribute this result to the very peaked gaussian profile typical of ICRF-driven ions, which in turn validates the approximations used to derive eq.[12]. Conversely, we notice a larger discrepancy between the results obtained solving eq.[12] and eq.[6] to the order $q=200$: nevertheless this difference is still within the uncertainty of the NPA measurement. However, the numerical solution of eq.[6] to the order $q=10$ and $q=200$ requires respectively 8 and 187 more computational time than eq.[12], therefore for practical purposes we have discarded these two methods in our further analysis.

4. VALIDATION OF THE NPA MEASUREMENTS OF N_0 AND T_0

Having inferred the peak fast ion density n_0 and temperature T_0 from KF1 measurements, it is now important to compare these results with other independent measurements and theories on ICRF heating to validate the method employed.

The simplest theoretical approach to model the distribution function of ICRF-driven minority high energy ions has been given by Stix [12] in 1975. He considered the balance between

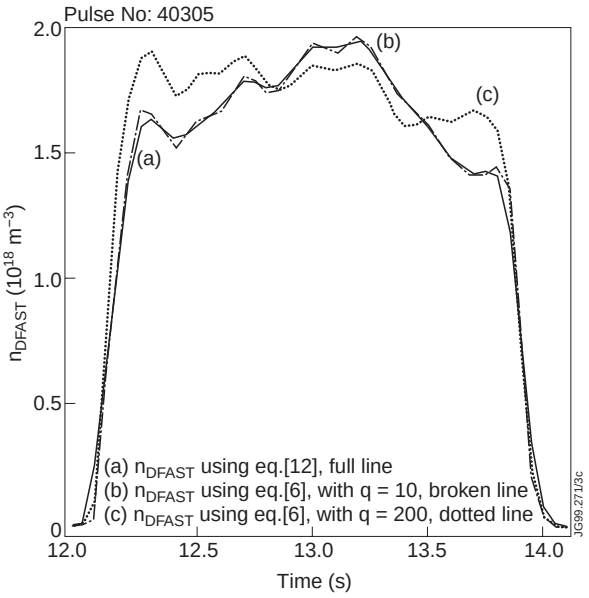

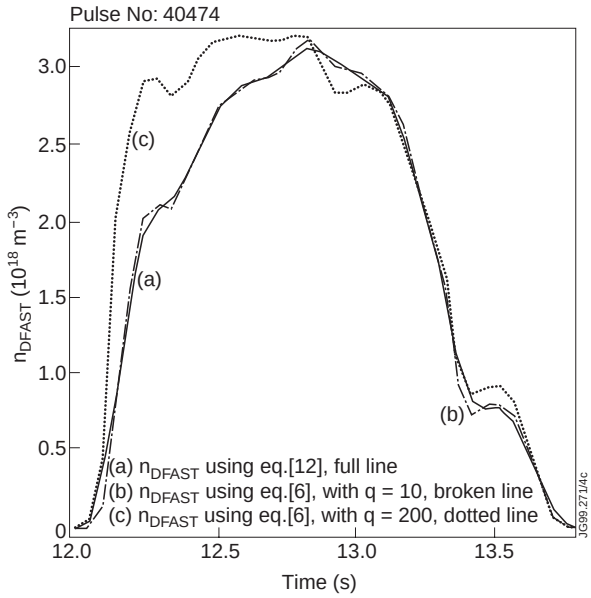

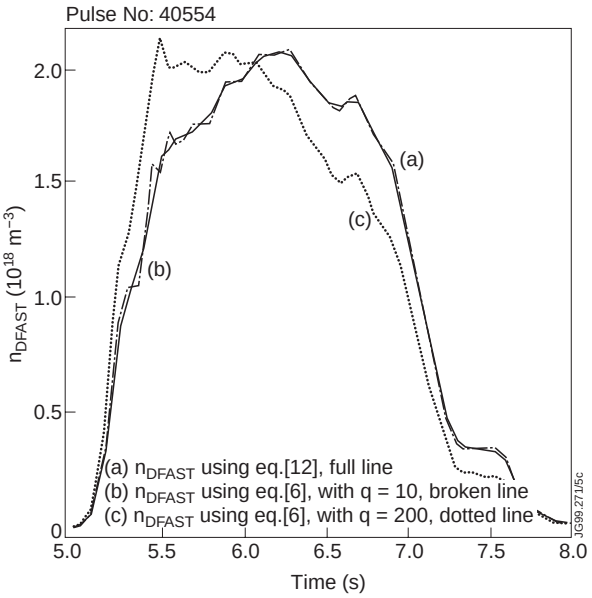

Fig.1: Comparison of the fast deuteron density n_{DFAST} inferred from NPA measurements during three combined ICRF+NBI heating plasma pulses: fig.1a shows results for #40305, fig.1b for #40474, fig.1c for #40554. We obtain three different numerical estimates: (a) by solving eq.[12] (full line), (b) by solving eq.[6] to the order q=10 (broken line), and (c) by solving eq.[6] to the order q=200 (dotted line). We notice that the largest discrepancy is well within the uncertainty in the measurement of the absolute atomic flux, typically ≈30% [6].

the resonant coercive force of the ICRF wave field and ion-electron collisional drag at energies such that ion-ion collisions are ineffective in changing the momentum of the ions. This occurs for ions at energies $E>>E_{CRIT}$, $E_{CRIT}=14.8A_iT_e[\Sigma n_jZ_j^2/n_eA_j]^{2/3}\approx 8.7T_e$: here T_e and n_e are the electron temperature and density, A and Z are the ion atomic number and nuclear charge, the subscript i and j refer respectively to resonant and non-resonant ion species, and the sum is intended over the latter. For typical JET ICRF heating experiments $T_e\approx 10keV$ and the energy range of the NPA measurements lies above E_{CRIT}. In this situation the fast ion distribution function is anisotropic, with $T_\perp >> T_{||}$, and slowing down acts as the only sink of perpendicular energy, since pitch-angle scattering is negligible. When steady-state conditions are reached, the fast ion energy density is $W_{FAST}=\Sigma n(T_\perp+T_{||}/2)=\Sigma\rho_{ABS}\tau_{SD}/2\approx\Sigma nT_\perp$. Here ρ_{ABS} is the ICRF power density absorbed by fast minority ions, τ_{SD} is the ion-electron slowing-down time and the sum is intended over resonant ion species. The Stix model does not necessarily imply that $T_\perp$ should

increase linearly with the ICRF input power P_{ICRF}, since the fraction of ICRF power, and hence ρ_{ABS}, which is coupled to the resonant ions is itself a non-linear function of P_{ICRF} [13,14]. However, one would expect that $T_\perp \approx (P_{ICRF})^{\nu}$, $\nu \approx 1$, if this non-linear dependence is weak. McClements et al. analysed in [5] ICRF heating of minority protons in deuterium plasmas: by using eq.[14] to obtain a set of values for T_0 they showed that $T_0 \approx (P_{ICRF})^{0.89 \pm 0.06}$. The scaling is almost exactly linear, and in this respect there is good agreement between the measurements and the Stix model.

Purpose of the present work is to extend the analysis of McClements et al. [5] by validating the absolute measurement of the ICRF-heated ion density. We consider ICRF heating of JET deuterium plasmas in the presence of two minority resonant ion species, background protons and high energy deuterons due to NBI. We use T_0 as given in eq.[14] and verify our result for n_0 against spectroscopic and low-energy NPA measurements of the fast ion density. Finally, we compute the fast ion perpendicular energy content using the above n_0 and T_0 and verify this results against independent magnetic measurements. In [15] and [16] we have shown how the measurements of n_0 and T_0 provide self-consistent interpretation of the ICRF-heated ion distribution functions in term of wave propagation and absorption during multispecies ICRF heating of JET deuterium plasmas.

During hydrogen minority ICRF heating of thermal low temperature deuterium plasmas, it is reasonable to assume [12] that a single bi-Maxwellian distribution function, with $T_{p\perp} >> T_{p||}$, describes the whole hydrogen population, since hydrogen heating occurs at the 1st cyclotron harmonic and 2nd harmonic deuterium heating is negligible in a thermal plasma with bulk ion temperature $T_D < 20keV$ [16]. Thus we can compare the proton density n_p inferred from the high energy NPA in the range $0.3 \le E(MeV) \le 1.5$, $n_{NPA,}$ eq.[15], with those inferred from the low energy NPA, n_{LOW}, for $E \le 160(keV)$, and from spectroscopic measurements of the thermal H_α / D_α line intensity ratio, n_{SPECT}. To this aim, we have computed n_{NPA}, n_{LOW} and n_{SPECT} for a number of ICRF-heating only plasma pulses, covering a wide range in plasma parameters, such as electron density and temperature, plasma current and toroidal magnetic field. Then we have averaged these results over the different plasma pulses to obtain meaningful statistics. In fig.2 we present the results of this analysis by showing the comparison between n_{NPA}, n_{LOW} and n_{SPECT} in the range

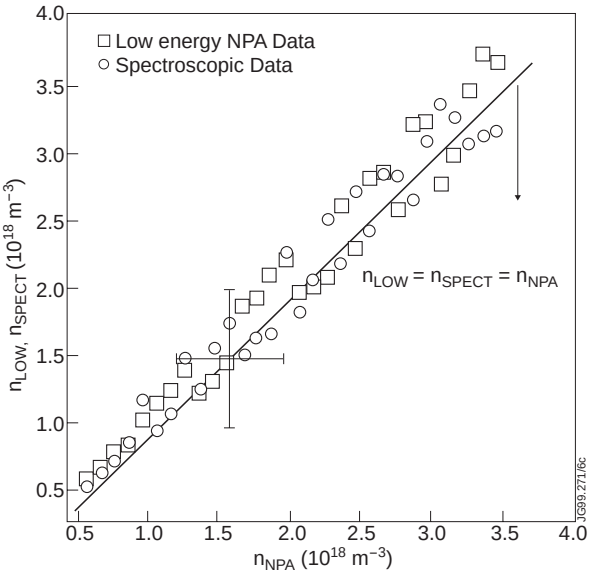

Fig.2: Comparison between the proton density n_p measured by the high energy NPA, n_{NPA}, the low energy NPA, n_{LOW} (symbol □), and the H_α/D_α line intensity ratio for ICRF heating plasma pulses, n_{SPECT} (symbol ○). The diagonal line indicates $n_{NPA}=n_{LOW}=n_{SPECT}$. For clarity, the error bars on the measurements are indicated just for one data point. We notice that these three measurements are very well correlated with each other in the entire range of the measurements, $0.6 \le n_p(10^{18}m^{-3}) \le 3.5$.

$0.6 \leq n_p(10^{18} m^{-3}) \leq 3.5$. It must be pointed out at this moment that these three measurements are not exactly equivalent: the energy range is different, the low energy NPA is a line-integrated measurement on the plasma mid-plane across the minor radius, and the H_α/D_α measurement is taken at the plasma edge. However, a strong correlation between the low energy NPA and the spectroscopic measurements has been previously established in JET [17]. We expect this to remain valid for the high energy NPA measurements unless the procedure we are using to infer the proton density is not correct. From fig.2 we notice a clear consistency between n_{NPA}, n_{LOW} and n_{SPECT}, with the larger discrepancy being within their typical uncertainties, estimated to be of the order ≈30%. Therefore we consider validated our method to infer the absolute proton density in the plasma centre from the NPA measurements.

Injection of high energy deuterium atoms, at *E=80keV* and *E=140keV*, into a thermal plasma is used in JET experiments to increase the bulk ion temperature through ion-ion collisions and to provide the source of donors required for active CX spectroscopy measurements. When ICRF heating is used together with beam injection, a fraction of ICRF power is absorbed by the beam deuterons through 2nd harmonic cyclotron heating. Using the intensity of the measured radiation it is possible to compute the density of the injected deuterons. In fig.3 we compare the fast deuteron density n_{DFAST} inferred from the high energy NPA, n_{NPA}, with that inferred from CX spectroscopy, n_{CX}, using the same procedure as for determining the proton density. Good quantitative agreement is found within the uncertainties of the measurements. However, we notice that n_{CX} is systematically larger than n_{NPA}: we attribute this result to the fact that not the entire population of injected deuterons undergoes ICRF diffusion in velocity space. Therefore the fast deuteron density in the energy range of the NPA measurements, *E≥287keV*, is lower than the total NBI-deuteron density.

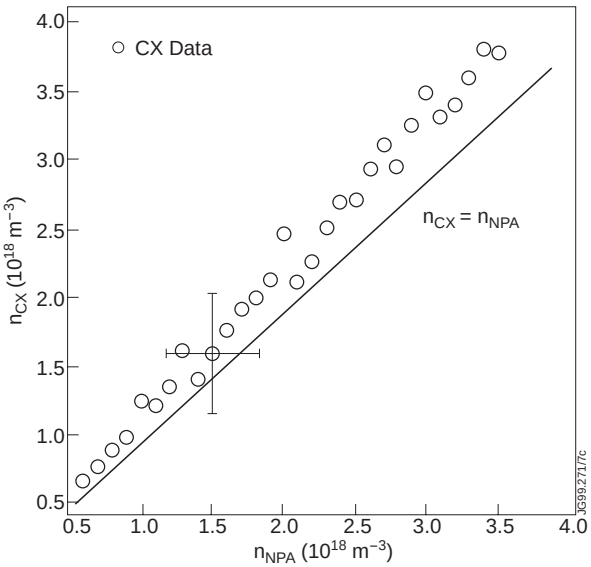

Fig.3: Comparison between the fast deuteron density n_{DFAST} measured by the high energy NPA, n_{NPA}, and by CX spectroscopy, n_{CX}, during combined ICRF+NBI heating experiments. The diagonal line indicates $n_{NPA}=n_{CX}$. For clarity, the error bars on the measurements are indicated just for one data point. We notice that these two measurements are very well correlated with each other in the entire range of the measurements, $0.6 \leq n_{DFAST}(10^{18} m^{-3}) \leq 3.5$. However, n_{CX} is systematically larger than n_{NPA}: we attribute this result to the fact that not the entire population of injected deuterons undergoes ICRF diffusion in velocity space and is driven to higher energies than those at which they are injected.

Finally, it is possible to estimate the perpendicular energy content of ICRF-heated fast ion populations by using a combination of magnetic measurements that put different weights on the parallel and perpendicular energy of the particles. We compute the

perpendicular fast ion energy density during combined ICRF+NBI heating plasma pulses at the 2nd deuterium cyclotron harmonic, following the method described in [15] and [16].

In [15] we have presented a method to solve the evolution equation for slowing-down NBI ions under the combined effects of collisions with electrons and diffusion due to the ICRF wave fields. We then computed the total fast ion energy content using a collisional energy balance, which includes only losses due to ion-electron collisions as in [5,6,12,15,16]

$$W_{FAST} = \sum_{FAST} \int dV_{PLASMA} \left[nT_{\perp} \left(1 + \frac{T_{||}}{2T_{\perp}} \right) \right]_{FAST} = W_{MAG} \ . \tag{16}$$

Here the sum is intended over the resonant ion species, and V_{PLASMA} is the plasma volume. We then compare the total energy content of the measured distribution functions W_{FAST} with the magnetic measurement W_{MAG}. A more difficult problem is related to the basic fact that 2nd harmonic deuterium heating coincides with 1st harmonic proton heating: thus we have two fast ion species, whereas the high energy NPA measures only one ion species at a time. For combined ICRF+NBI heating experiments we routinely measure the fast deuteron distribution function: thus we model the proton population with a bi-Maxwellian distribution function using independent measurements of n_p/n_D, and energy equi-partition for the proton parallel and perpendicular temperatures. Therefore we obtain as in [6,15,16]

$$T_{\perp p} = T_{DBULK} + \sqrt{\frac{m_D}{m_p}} \frac{W_e}{W_{DBULK} + W_{DFAST}} T_{\perp DFAST} \ , \ T_{||p} = \frac{k_{||}^2}{k_{\perp}^2} T_{\perp p} \ .$$

Here W_e, W_{DBULK} and W_{DFAST} are respectively the electron, bulk and fast deuteron energy density, $k_{||}$ and $k_{\perp}$ are the ICRF wave parallel and perpendicular wavenumbers. We computed W_{FAST} and W_{MAG}, for the above combined heating experiments, and the results are shown respectively in fig.4a for #40305, in fig.4b for #40474 and in fig.4c for #40554, together with the applied beam (P_{NBI}) and ICRF (P_{ICRF}) heating power. We notice that the time evolution of W_{FAST} and W_{MAG} follows closely the additional heating, confirming the assumptions made in our calculation, and there is an excellent quantitative agreement between W_{FAST} and W_{MAG} within the uncertainties of the NPA and magnetic measurements.

5. CONCLUSIONS

High energy NPA measurements are routinely used in JET to deduce the energy distribution functions of different ions in the range $0.3 \leq E(MeV) \leq 3.5$. Previous work [5] demonstrated that the perpendicular temperature of ICRF heated protons deduced from NPA measurements is in good accord with the well-established Stix theory [12,14] and the magnetic measurements of the fast ion energy content when the proton density is taken from independent measurements.

In this paper we have extended the previous work of McClements et al. [5] to determine the density of resonant ion species, with the aim to provide self-consistent interpretation of the

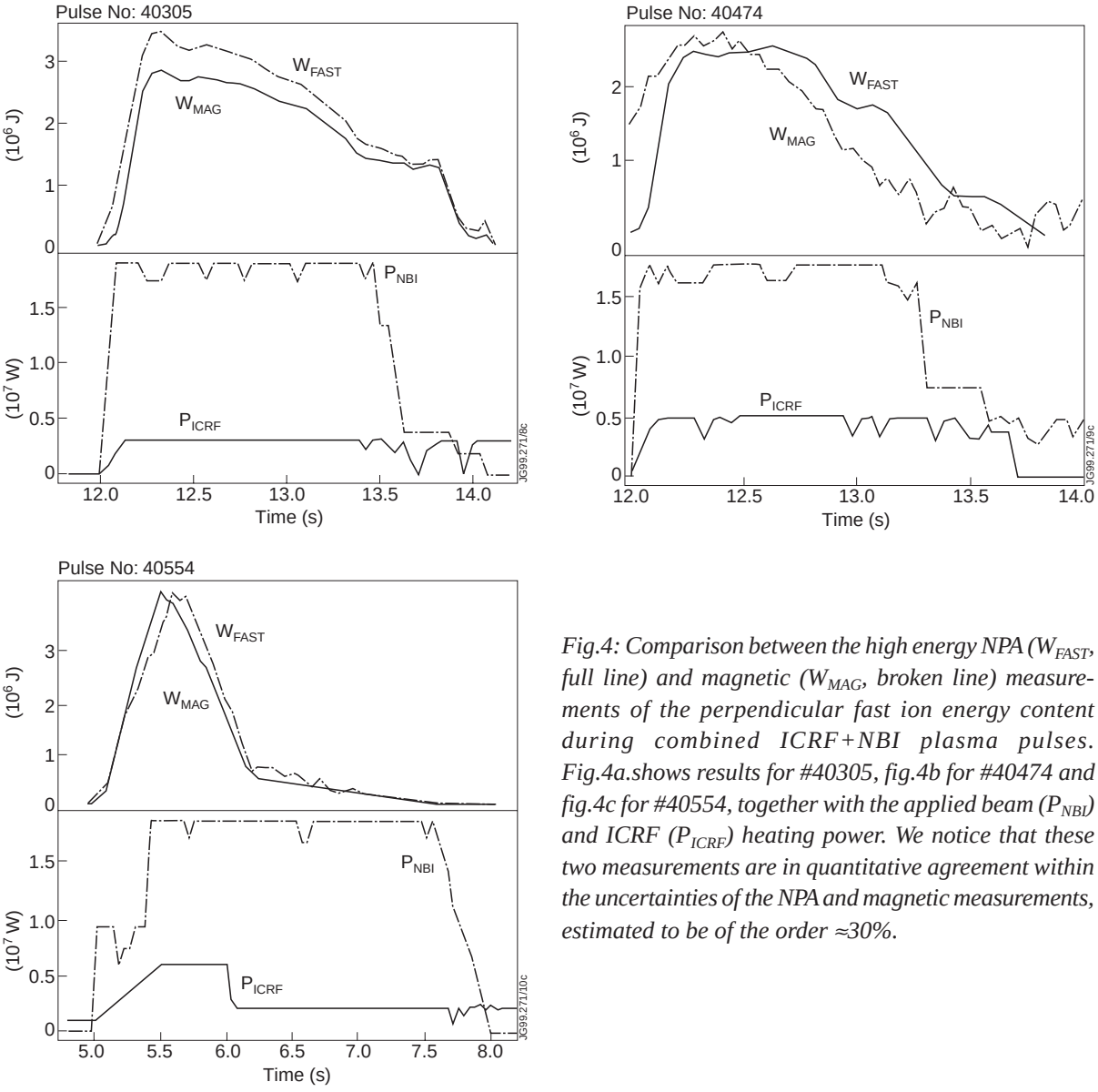

Fig.4: Comparison between the high energy NPA (W_{FAST}, full line) and magnetic (W_{MAG}, broken line) measurements of the perpendicular fast ion energy content during combined ICRF+NBI plasma pulses. Fig.4a.shows results for #40305, fig.4b for #40474 and fig.4c for #40554, together with the applied beam (P_{NBI}) and ICRF (P_{ICRF}) heating power. We notice that these two measurements are in quantitative agreement within the uncertainties of the NPA and magnetic measurements, estimated to be of the order ≈30%.

absolute magnitude of the fast ion distribution function during combined ICRF+NBI heating experiments. We have developed an analytic calculation to infer the absolute fast ion density in the plasma centre by unfolding the NPA measurement, which is line-integrated along the line-of-sight and volume-averaged in the observation solid angle.

Applying to combined ICRF+NBI heating experiments where two minority resonant ion species, hydrogen and beam deuterons, are present, we have shown that (a) the absolute fast ion density measured by the NPA agrees well with independent spectroscopic and low energy NPA measurements of the two species, and that (b) the energy content of the resonant ions determined self-consistently using the NPA measurements is in agreement with independent magnetic measurements of the total fast ion energy content.

These results further contribute to validating the IIN model [8], which forms the basis for the interpretation of these NPA measurements. In addition to that, we have successfully applied

the analytic tools developed in this paper to the interpretation of measurements of hydrogen isotope ion distribution functions during multispecies minority ICRF heating experiments in the JET tokamak [15,16].

ACKNOWLEDGEMENTS

The authors would like to thank Professor Malcolm Haines for support and encouragement of this work. We are indebted to Dr.Klaus-Dieter Zastrow and Klaus Guenther for careful analysis of spectroscopic and low energy NPA measurements in support of this work.

REFERENCES

[1} Heidbrink,W.W., Sadler, G., JET Laboratory Report **JET-P(93)63** 1993.

[2] I.H.Hutchinson, *Principles of Plasma Diagnostics*, Cambridge University Press, Cambridge, UK, 1987.

[3] Start, D.F.H., et al., Phys. Rev. Lett. **80** (1998) 4681.

[4] Eriksson, L.-G., et al., Phys. Rev. Lett. **81** (1998) 1231.

[5] McClements, K.G., Dendy, R.O., Gondhalekar, A., Nucl. Fus. **37** (1997) 473.

[6] D.Testa, *Ph.D. Thesis*, The Blackett Laboratory, Imperial College of Science, Technology and Medicine, London, UK, 1998.

[7] Korotkov, A.A., Gondhalekar, A, Akers, R.J., JET Laboratory Report **JET-P(98)25** 1998.

[8] Korotkov, A.A., Gondhalekar, A., Stuart, A.J., Nucl. Fusion **37** (1997) 35.

[9] Coppi, B., et al., F., Phys. Fluids **29** (1986) 4060.

[10] White, R.B., et al., Phys. Rev. Lett. **60** (1988) 2038.

[11] Izvozchikov, A.B., et al., JET Laboratory Report **JET-R(91)12** 1991,

[12] Stix, T.H., Nucl. Fusion **15** (1975) 737.

[13] Eriksson, L.-G., Hellstein, T., Phys. Sc. **52** (1995) 70.

[14] Stix, T.H., *Waves in Plasma*, American Institute of Physics, New York, USA, 1992.

[15] Testa, D., Core, W.G.F., Gondalekhar, A., *Ion Cyclotron Resonance Frequency heating of deuterium plasmas in the Joint European Torus: modelling of the resonant minority ion distribution function*, Physics of Plasmas, **6** (1999), 3489.

[16] Testa, D., Core, W.G.F., Gondalekhar, A., *Ion Cyclotron Resonance Frequency heating of deuterium plasmas in the Joint European Torus: interpretation of measurements of minority hydrogen isotope ion distribution functions*, Physics of Plasmas, **6** (1999), 3498.

[17] Bracco, G., Guenther, K., JET Laboratory Report **JET-R(96)04** 1996.